Accepted Manuscript

A novel atom search optimization for dispersion coefficient estimation in groundwater

Weiguo Zhao, Liying Wang, Zhenxing Zhang

PII: S0167-739X(18)30657-5
DOI: https://doi.org/10.1016/j.future.2018.05.037
Reference: FUTURE 4212

To appear in: *Future Generation Computer Systems*

Received date : 23 March 2018
Revised date : 20 April 2018
Accepted date : 17 May 2018

Please cite this article as: W. Zhao, L. Wang, Z. Zhang, A novel atom search optimization for dispersion coefficient estimation in groundwater, *Future Generation Computer Systems* (2018), https://doi.org/10.1016/j.future.2018.05.037

This is a PDF file of an unedited manuscript that has been accepted for publication. As a service to our customers we are providing this early version of the manuscript. The manuscript will undergo copyediting, typesetting, and review of the resulting proof before it is published in its final form. Please note that during the production process errors may be discovered which could affect the content, and all legal disclaimers that apply to the journal pertain.

ACCEPTED MANUSCRIPT

A Novel Atom Search Optimization for Dispersion Coefficient Estimation in Groundwater

Weiguo Zhao[a,b], Liying Wang[a,*], Zhenxing Zhang[b]

a. School of Water Conservancy and Hydropower, Hebei University of Engineering, Handan, Hebei, 056021, China

b. Illinois State Water Survey, Prairie Research Institute, University of Illinois at Urbana-Champaign, Champaign, IL 61820, USA

*Corresponding author.

E-mail addresses: wgzhao@illinois.edu (W. Zhao), wangliying@hebeu.edu.cn (L. Wang), zhang538@illinois.edu (Z. Zhang)

Abstract: A new type of meta-heuristic global optimization methodology based on atom dynamics is introduced. The proposed Atom Search Optimization (ASO) approach is a population-based iterative heuristic global optimization algorithm for dealing with a diverse set of optimization problems. ASO mathematically models and mimics the atomic motion model in nature, where atoms interact with each other through interaction forces resulting form Lennard-Jones potential and constraint forces resulting from bond-length potential, the algorithm is simple and easy to implement. ASO is applied to a dispersion coefficient estimation problem, the experimental results demonstrate that ASO can outperform other well-known approaches such as Particle Swarm Optimization (PSO), Genetic Algorithm (GA) or Bacterial Foraging Optimization (BFO) and that ASO is competitive with its competitors for parameter estimation problems.

Keywords: Dispersion coefficient; parameter estimation; Global optimization; Particle swarm optimization; Genetic algorithm; Atom search optimization; Bacterial foraging optimization

1. Introduction

Nature containing boundless secrets is rich and fantastic, it brings a great deal of inspiration to people which can greatly contribute to social development. Intelligent algorithms (IAs) dealing with difficult problems in science and engineering is an important branch of the inspiration from nature. Since 1970s, a variety of nature-inspired optimization algorithms have been put forward and applied to many real-world problems [1,2,3,4], which consist of two basic characteristics. Firstly, they mimic evolving properties and living habit of biological systems. There are three most representative algorithms. Genetic algorithm (GA) [5] is a well-known classic optimization algorithm which can generally obtain high-quality solutions using mutation, crossover and selection steps, and it turned out to be a good global optimization approach. Particle swarm optimization (PSO) [6], which mimics social behaviors of bird flock. In PSO, every agent moves around the search space to improve its solution, and their personal best positions and the globally best position found so far are reserved by which their positions are updated locally and socially. Ant colony optimization (ACO) [7], as another well-known optimization method, which simulates foraging behaviors of real ant colonies. Essentially, ants communicate with each other by

ACCEPTED MANUSCRIPT

pheromone trails through path formation, which assists them to find the shortest path signifying a near-optimum solution. With their increasing popularity [8,9,10], quite a number of other similar algorithms in the literature are developed, including evolutionary strategies (ES) [11], differential evolution (DE) [12], evolutionary programming (EP) [13], memetic algorithm (MA) [14], bacterial foraging optimization (BFO) [15], biogeography-based optimization (BBO) [16], cuckoo search (CS) algorithm [17], artificial bee colony (ABC) [18], fruit fly optimization algorithm (FOA) [19], etc.

Another basic characteristic of nature-inspired algorithms is that some of them are enlightened from physical laws of different substances, among which, simulated annealing (SA) [20] is one of the most well-known algorithms, being inspired from the annealing process used in physical material in which a heated metal cools and freezes into a crystal texture with the minimum energy. Along with DE, there are many others developed and successfully performed including electromagnetism-like mechanism (EM) [21] based on attraction-repulsion mechanism of electromagnetism, central force optimization (CFO) [22] and gravitational search algorithm (GSA) [23] both inspired from Newton's gravitational law, hysteretic optimization (HO) [24] enlightened inspired from demagnetization process, Big Bang-Big Crunch (BB-BC) [13] inspired from hypothesis of creation and destruction processes of the universe, wind driven optimization (WDO) [25] based on the earth's atmosphere motion, etc. Despite emerging many new optimization approaches, there is no any one which can perform the best over all different types of problems [26].

Groundwater environmental impact assessment is an important part of water environmental impact assessment, it mainly emphasizes on the prediction and evaluation of discharge or recharge water quality for groundwater quality impact to control or prevent the occurrence of groundwater pollution [27,28,29]. The prediction and evaluation for groundwater is to establish necessary mathematical models for water quality, and hydrodynamic dispersion coefficients are crucial and essential parameters for establishing the models [30, 31, 32]. So groundwater dispersion coefficients are very important parameters which characterize the motion and spread of pollutants in groundwater [33,34], consequently, it is vital for the accuracy of groundwater dispersion coefficient which has a direct impact on the accuracy of mathematical simulations and the authenticity of change prediction for groundwater quality. The numerical model is used to simulate hydrogeological process whose result largely depends on the hydrogeological parameters such as the permeability coefficient, the specific yield and so on, however, the field acquisition for the parameters is usually very expensive and time-consuming, and they can not reflect the parameters characteristics of the aquifer [35,36]. Aiming at this question, in recent years, many researchers start to utilize different optimization methods to inversely estimate hydrogeological coefficient with varying degrees of success [37, 38, 39]. Based on these successful applications of the existing nature-inspired optimization techniques, in this paper, an entirely novel optimization algorithm named atom search optimization (ASO) is proposed, which is successfully applied to dispersion coefficient estimation of groundwater, and the experiment results illustrate its superiority over its competitors.

The remainder of this paper is organized as follows. Section 2 describes ASO algorithm along with the underlying physical equations of atomic motion in detail. Section 3 introduces the model of dispersion coefficient estimation in groundwater. The application of ASO for a hydrogeologic parameter estimation problem is given in Section 4. Section 5 presents some

conclusions and suggestions.

2. Atom Search Optimization

All substances are made of atoms which are moving all the time, and atomic motion follows the classical mechanics [40]. According to Newton's second law, suppose that the force F_i is an interaction force and G_i *is* a constraint force together jointly acted on the *i*th atom in an atom system, then its acceleration related to its mass m_i an be given as follows [41]

$$a_i = \frac{F_i + G_i}{m_i} \tag{1}$$

The Lennard-Jones potential (L-J) potential is used as the interaction force acting on the *i*th atom from the *j*th atom in the *d*th dimension at *t* time, which can be written as

$$F_{ij}^{d}(t) = \frac{24\varepsilon(t)}{\sigma(t)}\left[2(\frac{\sigma(t)}{r_{ij}(t)})^{13} - (\frac{\sigma(t)}{r_{ij}(t)})^{7}\right]\frac{r_{ij}(t)}{\boldsymbol{r}_{ij}^{d}(t)} \tag{2}$$

and

$$F_{ij}^{'}(t) = \frac{24\varepsilon(t)}{\sigma(t)}\left[2(\frac{\sigma(t)}{r_{ij}(t)})^{13} - (\frac{\sigma(t)}{r_{ij}(t)})^{7}\right] \tag{3}$$

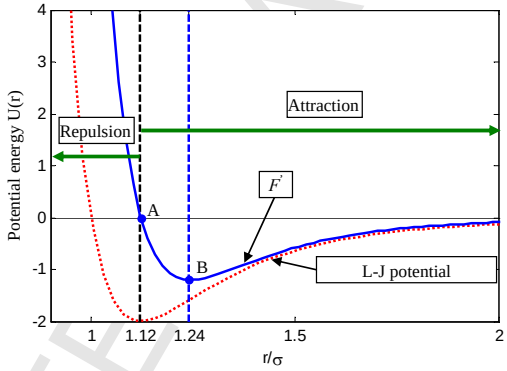

Fig. 1 Atoms force curve

The force curve of atoms for molecular dynamics is shown in Fig. 1. It can be seen that atoms keep a relative distance varying in a certain range all the time due to the repulsion or the attraction, and the change amplitude of the repulsion relative to the equilibration distance (r=1.12σ) is much greater than that of the attraction. The attraction is negative and the repulsion is positive, thus atoms would not be convergent to a specific position. So, equation (3) cannot be used directly to solve optimization problems. A revised version of this equation is developed as follows

$$F_{ij}^{'}(t) = -\eta(t)\left[2(h_{ij}(t))^{13} - (h_{ij}(t))^{7}\right] \tag{4}$$

where $\eta(t)$ is the depth function to adjust the repulsion region or the attraction region, which can be defined as

$$\eta(t) = \alpha(1 - \frac{t-1}{T})^{3} e^{-\frac{20t}{T}} \tag{5}$$

where *a* is the depth weight and *T* is the maximum number of iterations. The function behaviors of $F^{'}$ with different values of η corresponding to the values of h ranging from 0.9 to 2 are

illustrated in Fig. 2. From the figure, for the different values of η, the repulsion occurs when the values of h are ranging from 0.9 to 1.12, the attraction occurs when h are between 1.12 and 2, and the equilibration occurs when $h=1.12$. The attraction gradually increases with the increase of h from the equilibration ($h=1.12$) and reaches a maximum ($h=1.24$) and then begins to decrease. The attraction is approximately equal to zero when h is greater than or equal to 2. Therefore, in ASO, to improve the exploration, a lower limit of the repulsion with a smaller function value is set to $h=1.1$ and an upper limit of attraction with a larger function value is set to $h=2.4$, so h is defined as

$$h_{ij}(t)=\begin{cases} h_{min} & \dfrac{r_{ij}(t)}{\sigma(t)} < h_{min} \\ \dfrac{r_{ij}(t)}{\sigma(t)} & h_{min} \le \dfrac{r_{ij}(t)}{\sigma(t)} \le h_{max} \\ h_{max} & \dfrac{r_{ij}(t)}{\sigma(t)} > h_{max} \end{cases} \tag{6}$$

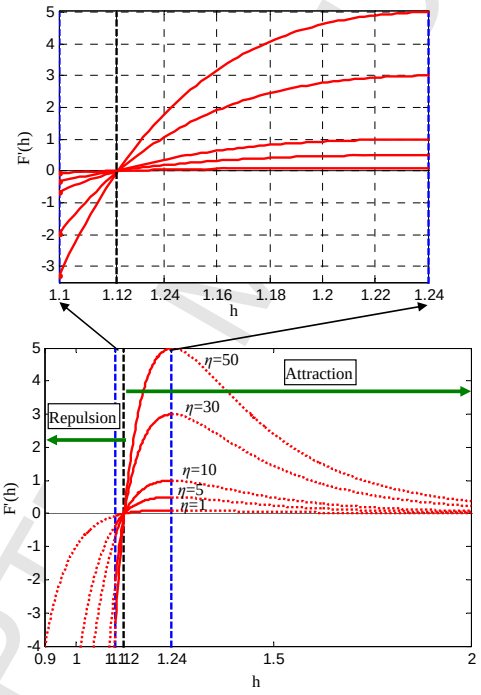

Fig. 2 Function behaviors of $F^{'}$ with different values of η

where h_{min} and h_{max} are a lower and an upper limits of h respectively, and the length scale $\sigma(t)$ is defined as

$$\sigma(t)=\left\| x_{ij}(t), \frac{\sum_{j\in Kbest} x_{ij}(t)}{K(t)} \right\|_2 \tag{7}$$

and

ACCEPTED MANUSCRIPT

$$\begin{cases} h_{min}=g_0+g(t) \\ h_{max}=u \end{cases} \tag{8}$$

where, *Kbest* is a subset of an atom population, which is made up of the first *K* atoms with the best function fitness values, *g* is the drift factor which can make the algorithm drift from the exploration to the exploitation, which is given as

$$g(t)=0.1\times\sin(\frac{\pi}{2}\times\frac{t}{T}) \tag{9}$$

Then the sum of components with random weights in the *d*th dimension acting on the *i*th atom from the other atoms can be considered as a total force, which is expressed as

$$F_i^d(t)=\sum_{j\in Kbest} rand_j F_{ij}^d(t) \tag{10}$$

where $rand_j$ is a random number in [0,1].

As Newton's third law implies, the force on the *j*th atom for the same pair-wise interaction is the opposite of the force on the *i*th atom

$$F_{ij}=-F_{ji} \tag{11}$$

The geometric constraint in molecular dynamics plays an important role in the motion of atoms. In ASO, for simplicity, suppose each atom has a covalence bond with the best atom, thus each atom is acted upon by a constraint force from the best atom**,** so the constraint of the *i*th atom can be rewritten as

$$\theta_i(t)=\left[\,|\,\boldsymbol{x}_i(t)-\boldsymbol{x}_{best}(t)\,|^2-b_{i,best}^2\right] \tag{12}$$

where $x_{best}(t)$ is the position of the best atom at the *t*th iteration, and $b_{i,best}$ is a fixed bond length between the *i*th atom and the best atom, hence the constraint force can be obtained

$$G_i^d(t)=-\lambda(t)\nabla\theta_i^d(t)=-2\lambda(t)(x_i^d(t)-x_{best}^d(t)) \tag{13}$$

where $\lambda(t)$ is the Lagrangian multiplier. Then making the substitution of $2\lambda\to\lambda$, and the constraint force can be redefined as

$$G_i^d(t)=\lambda(t)(x_{best}^d(t)-x_i^d(t)) \tag{14}$$

The Lagrangian multiplier is defined as

$$\lambda(t)=\beta e^{-\frac{20t}{T}} \tag{15}$$

where β is the multiplier weight.

Therefore, the acceleration of the *i*th atom at time *t* can be written as

$$a_i^d(t)=\frac{F_i^d(t)}{m_i^d(t)}+\frac{G_i^d(t)}{m_i^d(t)}=-\alpha(1-\frac{t-1}{T})^3 e^{-\frac{20t}{T}}\sum_{j\in Kbest}\frac{rand_j\left[2\times(h_{ij}(t))^{13}-(h_{ij})^7\right]}{m_i(t)}$$
$$\frac{(x_i^d(t)-x_i^d(t))}{\|\boldsymbol{x}_i(t),\boldsymbol{x}_j(t)\|_2}+\beta e^{-\frac{20t}{T}}\frac{x_{best}^d(t)-x_i^d(t)}{m_i(t)} \quad (16)$$

where $m_i(t)$ is the mass of the *i*th atom at the *t*th iteration, which can be measured, at the simplest level, by its function fitness value. The better a function fitness value is, the bigger mass the atom has, which can reduce its acceleration. The mass of the *i*th atom can be calculated as

$$M_i(t)=e^{-\frac{Fit_i(t)-Fit_{best}(t)}{Fit_{worst}(t)-Fit_{best}(t)}} \quad (17)$$

$$m_i(t)=\frac{M_i(t)}{\sum_{j=1}^{N}M_j(t)} \quad (18)$$

For a minimum problem, where $Fit_{best}(t)$ and $Fit_{worst}(t)$ are the atoms with the minimum fitness value and the maximum fitness value at the *t*th iteration respectively, $Fit_i(t)$ is the function fitness value of the *i*th atom at the *t*th iteration, and, $Fit_{best}(t)$ and $Fit_{worst}(t)$ are expressed as

$$Fit_{best}(\mathrm{t})=\min_{i\in\{1,2,\cdots,N\}}Fit_i(t) \quad (19)$$

$$Fit_{worst}(\mathrm{t})=\max_{i\in\{1,2,\cdots,N\}}Fit_i(t) \quad (20)$$

To simplify the algorithm, the position and the velocity of the *i*th atom at (*t*+1)th iteration can be denoted as follows

$$v_i^d(t+1)=rand_i^d v_i^d(t)+a_i^d(t) \quad (21)$$

$$x_i^d(t+1)=x_i^d(t)+v_i^d(t+1) \quad (22)$$

In ASO algorithm, to enhance the exploration in the first stage of iterations, each atom needs to interact with as many atoms as possible with the better fitness value as its *K* neighbors. To enhance the exploitation in the final stage of iterations, the atoms need to interact with as few atoms as possible with the better fitness value as its *K* neighbors. In particular, whether the interaction force acting on each atom from each of its neighbors is attraction or repulsion will depend on the ratio of the distance r_{ij} to the length scale σ, and the length scale σ **r**epresents the distance from each atom to the average position of its *K* neighbors. So, *K* is a function of time, which gradually decreases with the lapse of iterations, and *K* can be calculated as

$$K(t)=N-(N-2)\times\sqrt{\frac{t}{T}} \quad (23)$$

ACCEPTED MANUSCRIPT

The forces of an atom population are shown in Fig. 3, in which the first 5 atoms with the best fitness value are regarded as the *KBest.* It can be seen from the figure, A_1, A_2, A_3 and A_4 compose the *KBest*. A_5, A_6 and A_7 attract or repel each atom in the *KBest,* A_1, A_2, A_3 and A_4 attract or repel each other. Each atom in the population, except for A_1 (x_{best}), has a constraint force from the best atom A_1.

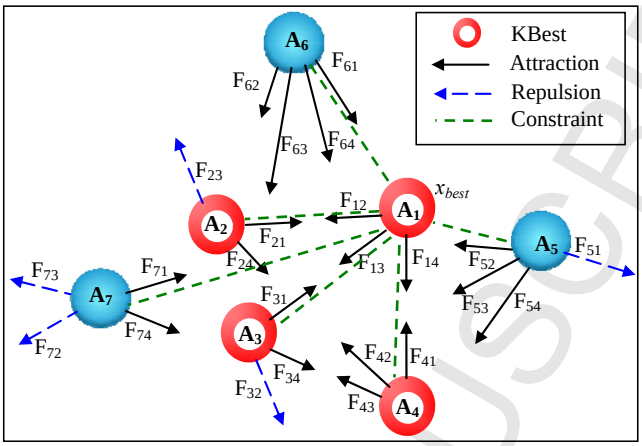

Fig. 3 Forces of an atom system with *KBest* for K=5

The pseudo code of ASO algorithm is provided in Fig. 4.

Randomly initialize a set of atoms X (solutions) and their velocity v, and Fit_{Best}=Inf.
While the stop criterion is not satisfied do
  For each atom X_i do
    Calculate the fitness value Fit_i;
    If $Fit_i < Fit_{Best}$ then
      $Fit_{Best} = Fit_i$;
      $X_{Best} = X_i$;
    End if.
    Calculate the mass using equations (8) and (9);
    Determine its K neighbors using equation (14);
    Calculate of the intraction force F_i and the constraint force G_i using equations (2) and (5) respectively;
    Calculate the acceleration using equation (7);
    Update the velocity using equation (12);
    Update the position using equation (13);
  End For.
End While.
Find the best solution so far X_{Best}.

Fig. 4 Pseudo code of ASO algorithm

3. Model of Dispersion Coefficient Estimation in Groundwater

Two-dimensional hydrodynamic dispersion is adopted in which the aquifer is uniform thickness, homogeneous and one-dimensional steady motion, the infinite plane is *xy* plane and the water flow is along the x coordinate. The tracer is injected when testing, it is put in instantaneously at t=0, and the origin of coordinates of observation wells is on the x-axis along the water flow. Therefore, the two-dimensional advection-dispersion equation of solute concentration

can be expressed as [42]

$$\frac{\partial C}{\partial t} = D_L \frac{\partial^2 C}{\partial x^2} + D_T \frac{\partial^2 C}{\partial y} - v\frac{\partial C}{\partial x} \tag{24}$$

The initial condition is

$$\int_{-\infty}^{\infty}\int_{-\infty}^{\infty} nC dxdy = m \tag{25}$$

The boundary condition is

$$\begin{cases} C(x, y, 0), x, y \neq 0 \\ C(\pm\infty, y, t) = 0 \\ C(x, \pm\infty, t) = 0 \\ t \geq 0 \end{cases} \tag{26}$$

where v is the linear velocity of flow in the x direction, $C(x,y,t)$ is the resident fluid solute concentration, x and y are the Cartesian coordinates, t is the time, D_L and D_T are the longitudinal and transverse hydrodynamic dispersion coefficients respectively, and n is the effective porosity of aquifer. The molecular diffusion effect of the tracer is less than 10^{-5} m^2/d and it can be neglected compared to the dispersion coefficients, so

$$\begin{cases} D_L = a_L v \\ D_T = a_L v \end{cases} \tag{27}$$

Where a_L and a_T are the the longitudinal and transversal dispersivities. When the instantaneous input of a mass m of solute, as a vertical line source at xy and t=0 in a uniform infinite flow field, is put into equation (24), so the solution can be expressed as

$$C(x, y, t) = \frac{m/n}{4\pi v t\sqrt{a_L \cdot a_T}} \cdot \exp\left[-\frac{(x - vt)^2}{4a_L vt} - \frac{y^2}{4a_T vt}\right] \tag{28}$$

Suppose (x, y) is the coordinates of a observation well, $C(t)$ is the concentration of the tracer changing over time, and C_{max} is the peak of the concentration change of $C(t)$, then the nondimensional transformation is introduced by

$$C_R = \frac{C}{C_{\max}} \tag{29}$$

$$t_R = \frac{v \cdot t}{a_L} \tag{30}$$

$$a = \left(\frac{x^2}{a_L{}^2} + \frac{y^2}{a_L a_T}\right)^{\frac{1}{2}} \tag{31}$$

By substituting equations (29), (30) and (31) into equation (28) we can get

$$C_R(t_R) = K t_R^{-1} \cdot \exp\left(-\frac{a^2 + t_R^2}{4t_R}\right) \tag{32}$$

ACCEPTED MANUSCRIPT

$$\begin{cases} K = t_{R\max} \cdot \exp(\dfrac{a^2 + t_{R_{mas}}^2}{4 \cdot t_{R_{\max}}}) \\ t_{R_{\max}} = \sqrt{4 + a^2} - 2 \end{cases} \tag{33}$$

It can be observed in equation (32) that the relation c_R-t_R only depends on the nondimensional parameter a, the different values of a correspond to a set of c_R-t_R data whose standard dispersion curves can be plotted. Fig. 5 shows a series of standard dispersion curves corresponding to different values of a. The measured points of the observation well in the main flow direction are compared with the standard curves, the value of a corresponding to a proximate dispersion curve whose coordinates are (x_1, 0) is obtained, so according to equation (31) we can obtain

$$a_L = \frac{x_1}{a} \tag{34}$$

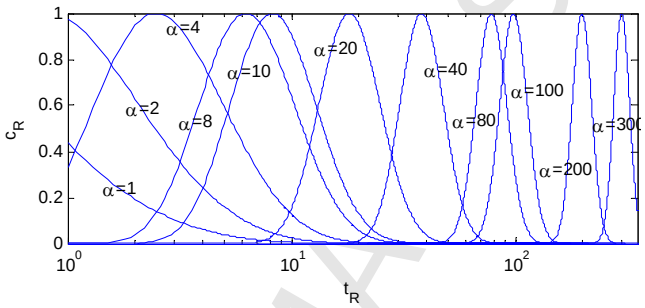

Fig. 5 Standard dispersion curves corresponding to different a

Meanwhile, the measured points of the observation well not in the main flow direction are compared with the standard curves, its corresponding value of a can be obtained and the coordinates of the well are (x_2, y_2), according to equation (8) we can obtain

$$a_T = \frac{y_2^2}{a_L(a^2 - \dfrac{x_2^2}{a_{1L}^2})} \tag{35}$$

By equation (28) the actual mean velocity can be expressed as

$$v = \frac{t_{R\max} \cdot a_L}{t_m} \tag{36}$$

The average flow velocity of groundwater (the actual velocity) can be got by:

$$v = \frac{n}{v_f} \tag{37}$$

Where v_f is the groundwater seepage velocity, and it can be measured in the single well by

$$v_f = \frac{\pi r}{2at} In \frac{C_a}{C_t} \tag{38}$$

4. Experimental analysis and discussions

4.1 Test data

ACCEPTED MANUSCRIPT

In this section, the proposed method is applied to dispersion coefficient estimation form a dispersion test that is kindly provided by [42]. Fig. 6 shows the arrangement of wells location, 0# injection well at the origin of coordinate is ϕ100 iron filter pipe, 1# and 2# observation wells are ϕ50 hard plastic filter pipe, the injected amount of the tracer is 10 millicuries, the radioactive intensity of the tracer dispersion is observed by a flow velocity and direction meter called *FD*-138, which is illustrated in Table 1.

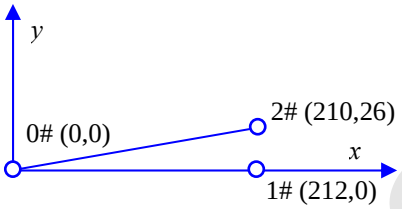

Fig. 6 Arrangement of well location

Table 1 Observation values of dispersion intensity

Observation time interval t (min)	1# observation well		2# observation well	
	Intensity N_r (mCi/h)	Normalized concentration change C_R	Intensity N_r (mCi/h)	Normalized concentration change C_R
188	44	0.017	-	-
198	200	0.077	16	0.012
203	360	0.14	-	-
208	760	0.29	40	0.031
218	1200	0.46	72	0.056
228	1900	0.73	128	0.10
238	2500	0.96	328	0.25
248	2600	1.00	688	0.53
258	2800	0.27	0.89	988
268	1800	0.69	-	-
278	1300	0.5	1288	1.00
288	700	0.27	988	0.77
14	380	0.15	668	0.52
18	200	0.085	408	0.32
24	140	0.054	268	0.21
30	52	0.020	108	0.084
40	36	0.014	52	0.040

4.2 Parameters Setup

In this section, to show the performance of ASO algorithm for dispersion coefficient estimation in groundwater, the experimental results are presented and different methods are employed including PSO, GA and BFO algorithms. The size of population and the maximum number of iterations are set to 30 and 200 respectively. To test the stability and effectiveness of the algorithms, every algorithm runs 30 times for the dispersion coefficient estimation experiments, and the results are based on the average performance.

The parameter settings for each algorithm are described as follows:

ASO: The depth weight a=50 and the multiplier weight β=0.2.

PSO: The nertia constant linearly decreases from 0.8 to 0.2, the cognitive constants c_1=2 and c_2=2.

GA: The election operator p_s is set by the roulette wheel method, the crossover operator p_c=0.4 and the mutation operator p_m=0.8.

BFO: The number of chemotactic steps N_c= 25, the swimming length N_s=4, the reproduction steps N_{re}=2, the elimination–dispersal events N_{ed}:=4, the elimination-dispersal with probability P_{ed}=0.25, and the size of the tumble step C=0.05.

The main purpose of the present research is to find a better value of a for an unknown standard dispersion curve to make the points of observation well fit a certain standard dispersion curve, so the objective function of dispersion test is to minimize the difference between the points of a observation well and a pending standard dispersion curve. The sum of squared errors (SSE) as fitting errors is usually used to an objective function in many literature.

NSE (Nash-Sutcliffe Efficiency) [43], as an evaluation criteria, is frequently used to evaluate the fitting effects of various simulation models based on parameter optimization methods which is expressed as

$$NSE = 1 - \frac{\sum_{i=1}^{n} (s_{obs,i} - s_{sim,i})^2}{\sum_{i=1}^{N} (s_{obs,i} - \overline{s}_{obs})^2} \tag{39}$$

where $s_{obs,i}$ is the observed value at time i; $s_{sim,i}$ is the simulated value at time i; $\overline{s}_{obs}$ is the average observed value，and n is the number of data. The best theoretical value of NSE is 1. In this work, the following objective function is adopted

$$\begin{aligned} \min f_{NSE}(\alpha_k) &= \sum_{k=1}^{m}\sum_{i=1}^{n} (C_R^{*,k}(t_i^k) - C_R^k(t_i^k))^2 \\ &= \sum_{k=1}^{m}\sum_{i=1}^{n} (C_R^{*,k}(t_i^k) - \frac{K}{t_i^k} \cdot \exp(-\frac{{\alpha_k}^2 + (t_i^k)^2}{4t_i^k}))^2 \end{aligned} \tag{40}$$

Subject to

$$0 \le \alpha_k \le 300, k = 1, \cdots, m \tag{41}$$

Where m is the number of observation well, t_i^k is the ith time interval of the kth observation well, C_R^{*k} is the concentration change of the tracer in the kth observation well, C_R^k is the concentration change of the tracer in the standard dispersion curve corresponding to the kth observation well. Obviously, The nearer the result of f_{NSE} approximates to zero， the better the fitting effect is.

To compare the convergence of different algorithms, there are two different performance evaluation indexes used to quantitatively compare these algorithms including the average of best-so-far solution and the standard deviation of best-so-far solution. The convergence processes of all comparative algorithms and the trajectories of a_1 and a_2 are shown in Fig. 7 and Fig. 8, respectively, and Table 2 describes the comparisons of optimization results. It can be observed that ASO has a faster convergence speed than the other algorithms from Fig. 7, which shows its advantage in terms of the convergence rate, meanwhile, from the final solutions in Table 2, it is

clear that the superiority of the standard deviation and the average demonstrates that ASO can achieve a better precision and performs more stable optimization than the others. In addition, form the trajectories of a_1 and a_2 in Fig. 8, for ASO, it can be seen that the trajectory curves have large-scale fluctuations frequently in the early iterations. With the lapse of iterations, such variation decreases in amplitude or frequency, and, the positions of atoms become monotonous and gradually tend to be stabilized to the global optimum in the later iterations. This behavior shows ASO performs a global search for the entire search space firstly and then performs a local search for a promising region.

Figs. 9-13 show the fitting results between the observation values and the standard dispersion curves acquired by the average identified dispersion coefficient obtained using different methods and Fig. 14 depicts the comparison of fitting effects of different methods, it can observed obviously that the dispersion curve obtained by the ASO is highly in coincidence with the observation values of the two wells compared with the other methods and it seems the fitting effects of ASO are better than BFO and [42]. However, it is difficult to visually identify the obvious fitting difference among ASO, PSO and GA owing to the similar precision, but it can be seen from Table 5, ASO is more competitive than its counterparts and its advantages are obvious in estimating dispersion coefficient in groundwater. Additionally, one can find that a bigger deviation has occurred between the observation values and the standard dispersion curves by the method in [42].

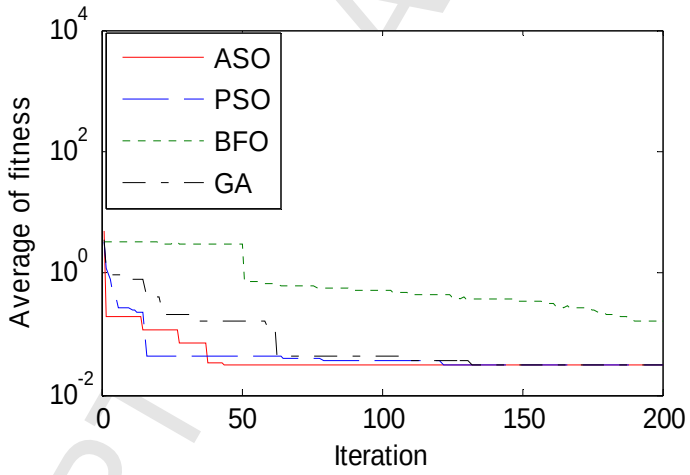

Fig. 7. Comparison of the average iteration process of different algorithms

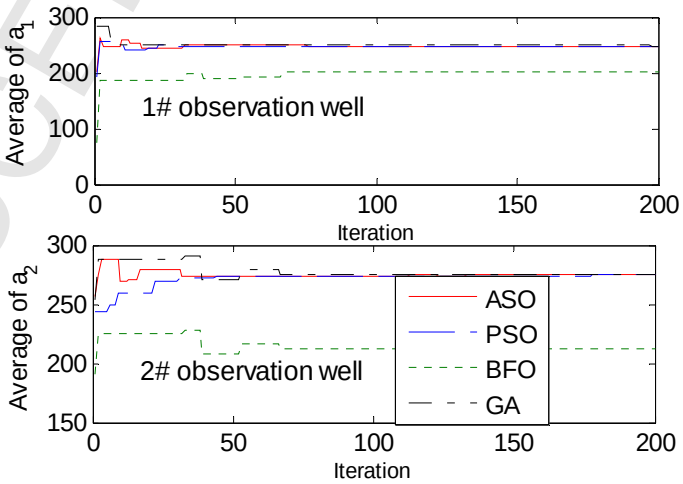

ACCEPTED MANUSCRIPT

Fig.8 Trajectories of a_1 and a_2 for algorithms

Table 2 Comparison results of objective function value for the two observation wells

Algorithms	f_{NSE}	
	Mean	Std
ASO	2.973×10^{-2}	7.7428×10^{-5}
PSO	2.978×10^{-2}	$7.4453\times10^{--2}$
GA	3.194×10^{-2}	4.6152×10^{-3}
BFO	0.1457	0.2142

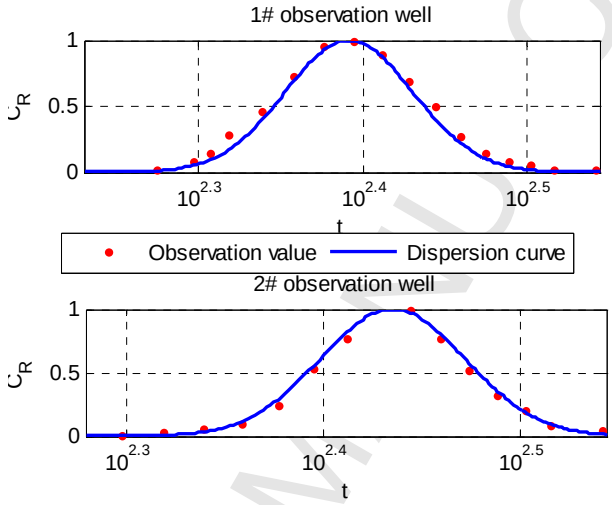

Fig. 9 Fitting results between the observation value and the standard dispersion curve acquired by ASO

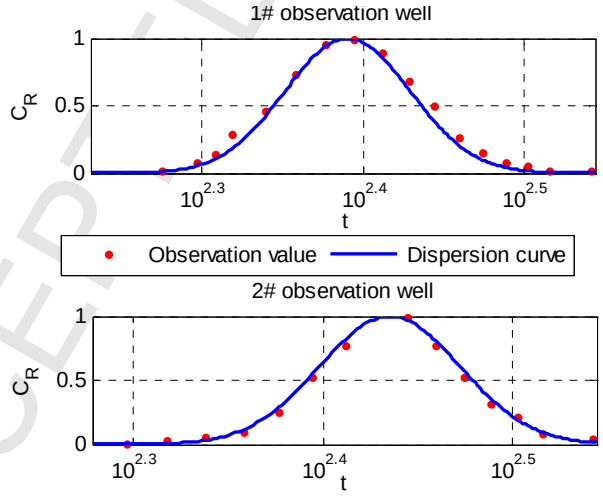

Fig. 10 Fitting results between the observation value and the standard dispersion curve acquired by PSO

ACCEPTED MANUSCRIPT

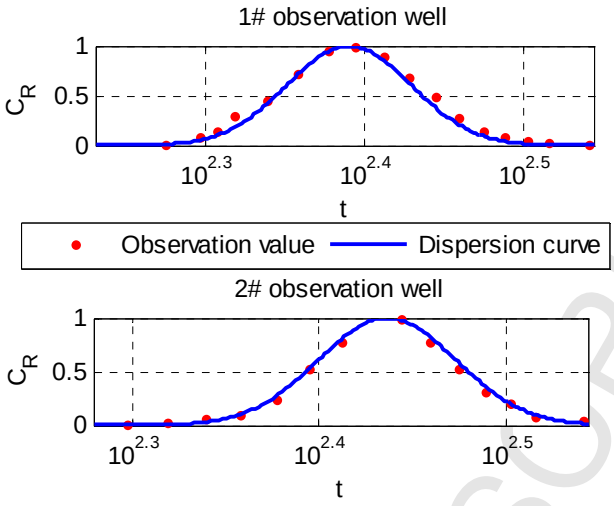

Fig. 11 Fitting results between the observation value and the standard dispersion curve acquired by GA

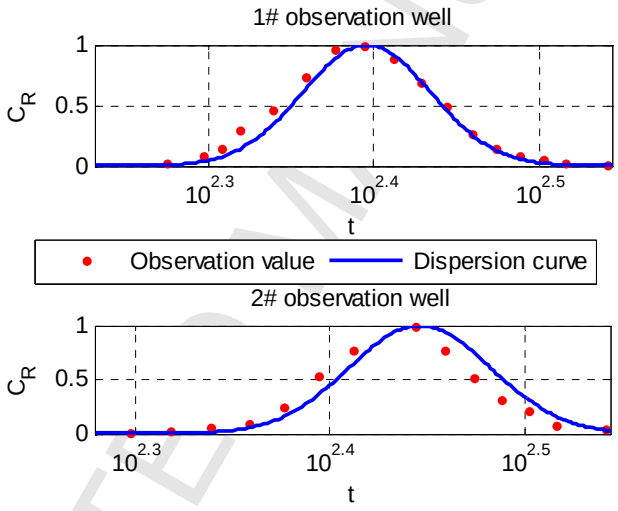

Fig. 12 Fitting results between the observation value and the standard dispersion curve acquired by BFO

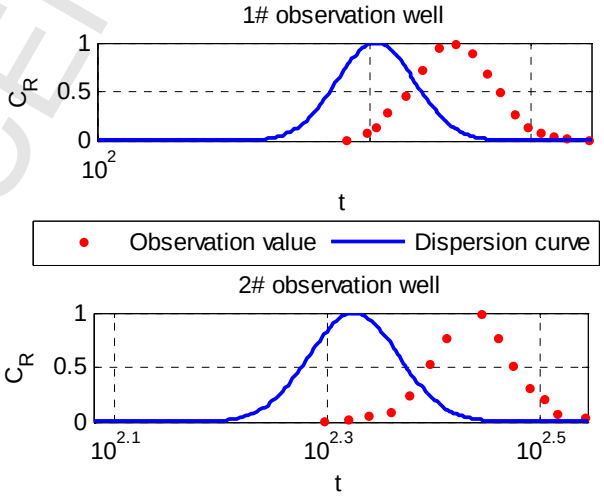

Fig.13 Fitting results between the observation value and the standard dispersion curve acquired by [42]

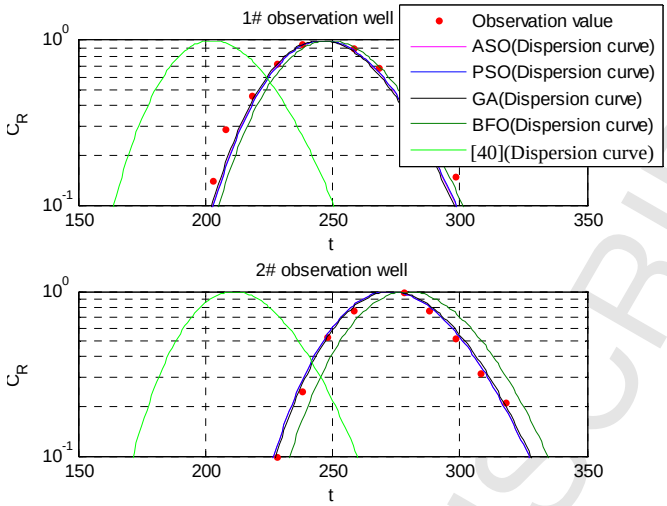

Fig. 14 Comparison of fitting results using different methods

When the nondimensional parameters a_1 and a_2 corresponding to different observation wells are given, the longitudinal coefficient D_L and transverse hydrodynamic dispersion coefficient D_T can be calculated. The statistics results of dispersion coefficient acquired by different methods are listed in Table 5 in detail, meanwhile, the curve fitting results of the observation wells by the different methods are also listed in Table 6 and Table 7 respectively, in addition, Fig. 15 also depicts the sum of squared errors (SSE) between the observation data and the data from the acquired standard dispersion curve, by comparing the SSE of PSO, GA, BFO, [42] and ASO, it can be observed that ASO can get smaller fitting errors than its competitors.

According to above comparison, it is clear that employing meta-heuristic algorithms such as PSO, GA, BFO and ASO can achieve better computational results. More importantly, among these algorithms, ASO can achieve the best computational results with its counterparts, thus demonstrating its highly flexibility and validity in estimating dispersion coefficient in groundwater.

Table 5 Statistics results of dispersion coefficient acquired by different methods

Coefficient		ASO	PSO	GA	BFO	[42]
a_1(#1)		248.1907	248.3612	247.5334	250.5741	204.64
a_2(#2)		274.3640	274.34919	275.12215	281.38411	213.1098
D_L		0.7149	0.7139	0.72066	0.7194	0.8150
D_T		4.465×10^{-2}	4.493×10^{-2}	4.266×10^{-2}	3.868×10^{-2}	1.188×10^{-2}
f_{NSE}	#1	2.136×10^{-2}	2.141×10^{-2}	2.218×10^{-2}	3.182×10^{-2}	2.0675
	#2	8.362×10^{-3}	8.3597×10^{-3}	9.768×10^{-3}	0.1139	2.6192

Table 6 Curve fitting results of 1# observation well by different methods

t	C_R	$C_R^{'}$				
		ASO	PSO	GA	BFO	[42]
188	0.017	0.0106	0.0104	0.0118	0.0073	0.7496
198	0.077	0.0519	0.0508	0.0562	0.0384	0.9728
203	0.14	0.0985	0.0967	0.1056	0.0757	0.9998
208	0.29	0.1705	0.1679	0.1811	0.1358	0.9659
218	0.46	0.3987	0.3943	0.4159	0.3391	0.7612

ACCEPTED MANUSCRIPT

228	0.73	0.6934	0.6886	0.7116	0.626	0.491
238	0.96	0.9313	0.9285	0.9415	0.8882	0.2658
248	1.00	0.9967	0.9973	0.9939	0.9997	0.1234
258	0.27	0.8728	0.8762	0.8593	0.917	0.05
268	0.69	0.6396	0.6441	0.6224	0.7015	0.018
278	0.5	0.3999	0.4038	0.3849	0.4564	0.0058
288	0.27	0.2169	0.2196	0.2066	0.2569	0.0017
14	0.15	0.1035	0.105	0.0977	0.1269	0.0005
18	0.085	0.044	0.0448	0.0412	0.0557	0.0001
24	0.054	0.0169	0.0172	0.0156	0.022	0
30	0.020	0.0059	0.006	0.0054	0.0079	0
40	0.014	0.0006	0.0006	0.0005	0.0008	0

Table 7 Curve fitting results of #2 observation well by different methods

t	C_R	$C_R^{'}$				
		ASO	PSO	GA	BFO	[42]
198	0.012	0.0009	0.0009	0.0008	0.0002	0.803
208	0.031	0.0066	0.0066	0.0059	0.0021	0.9883
218	0.056	0.0328	0.0329	0.0298	0.0128	0.9467
228	0.10	0.1135	0.1137	0.1053	0.054	0.7295
238	0.25	0.2864	0.2867	0.2708	0.1631	0.4649
248	0.53	0.547	0.5474	0.5266	0.3676	0.2507
258	988	0.8174	0.8177	0.7997	0.6398	0.1167
278	1.00	0.9717	0.9716	0.9787	0.9982	0.0173
288	0.77	0.8077	0.8074	0.8242	0.9373	0.0057
14	0.52	0.5741	0.5737	0.593	0.7464	0.0017
18	0.32	0.3543	0.354	0.3701	0.5123	0.0005
24	0.21	0.1924	0.1922	0.2031	0.3073	0.0001
30	0.084	0.093	0.0929	0.0992	0.1631	0
40	0.040	0.016	0.0159	0.0174	0.0332	0

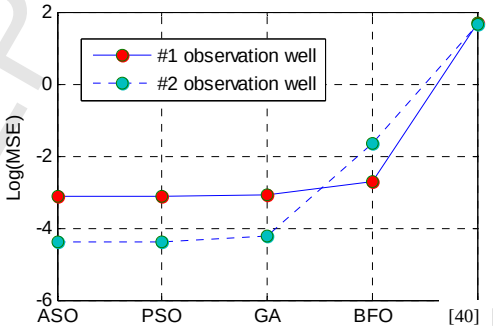

Fig. 15 Comparison of MSE using different methods

5. Conclusions

In this study, we have developed a novel meta-heuristic global optimization approach named atom search optimization (ASO). ASO is derived from the basic molecular dynamics governing the atomic motion which is based on the interaction and constraint forces. In ASO, each atom is

ACCEPTED MANUSCRIPT

acted on by the attractive or repulsive forces from its neighbors and the constraint force from the atom with the best fitness value, and the atomic motion follows Newton's second law. The attractive force encourages atoms to explore the entire search space extensively, and the repulsive force enables them to intensively exploit the promising regions. To illustrate the simplicity and availability of ASO, we present a dispersion coefficient estimation problem which is compared with its counterparts. The experimental results suggest that ASO is effective at optimizing dispersion coefficient in groundwater and that it is a promising alternative to PSO, GA and BFO extensively used in many real-world problems.

Acknowledge

This work is supported in part by Natural Science Foundation of Hebei Province of China (E2018402092, F2017402142), High-Level Talent Funding Project of Hebei Province of China (B2017003014), and Scientific Research Key Project of University of Hebei Province of China (ZD2017017).

References

[1] A.A. Ayman, Pid parameters optimization using genetic algorithm technique for electrohydraulic servo control system, Intell. Control Autom. 2 (2011) 888-896.
[2] G. Kourakos, A. Mantoglou, Development of a multi-objective optimization algorithm using surrogate models for coastal aquifer management, J. Hydrol. 479 (2013) 13-23.
[3] L. Poli, P. Rocca, L. Manica, A. Massa, Handling sideband radiations in time-modulated arrays through particle swarm optimization, IEEE Trans. Antennas Propag. 58(4) (2010) 1408-1411.
[4] W. Zhao, L. Wang, An effective bacterial foraging optimizer for global optimization, Inf. Sci. 329 (2016) 719-735.
[5] J.H. Holland, Adaptation in natural and artificial systems, University of Michigan Press, Ann Arbor, 1975.
[6]J. Kennedy, R. Eberhart, Particle swarm optimization, in: Proceedings of IEEE International Conference on Neural Networks, 1995, pp. 1942-1948
[7] M. Dorigo, V. Maniezzo, A. Colorni, Ant system: optimization by a colony of cooperating agents, IEEE Trans. Syst. Man Cybern. Part B 26(1) (1996) 29-41.
[8] K. Deepa Thilak, A. Amuthan, Cellular Automata-based Improved Ant Colony-based Optimization Algorithm for mitigating DDoS attacks in VANETs, Future Gener. Comput. Syst. 82 (2018) 304-314.
[9] H. Shahabinejad, M. Sohrabpour, A novel neutron energy spectrum unfolding code using particle swarm optimization, Radiat. Phys. Chem. 136 (2017) 9-16.
[10**] C.**Lai, Q. Shao, X. Chen, Z. Wang, X. Zhou, , B. Yang, L. Zhang, Flood risk zoning using a rule mining based on ant colony algorithm, J. Hydrol. 542 (2016) 268-280.
[11] H.G. Beyer, H.P. Schwefel, Evolution strategies-A comprehensive introduction, Nat. Comput. 1(1) (2002) 3-52.
[12] P. Rocca, G.. Oliveri, A. Massa, Differential evolution as applied to electromagnetics, IEEE Antennas Propag. Mag. 53(1) (2011) 38-49.
[13] K.A. Juste, H. Kita, E. Tanaka, J. Hasegawa, An evolutionary programming solution to the unit commitment problem, IEEE Trans. Power Syst. 14(4) (1999) 1452-1459.
[14] P. Moscato, A. Mendes, R. Berretta, Benchmarking a memetic algorithm for ordering microarray data, Biosyst. 88(1) (2007) 56-75.
[15] K.M. Passino, Biomimicry of bacterial foraging for distributed optimization and control, IEEE Control Syst. 22(3) (2002) 52-67.
[16] D. Simon, Biogeography-based optimization, IEEE Trans. Evol. Comput. 12(6) (2009) 702-713.
[17] X.S. Yang, S. Deb, Cuckoo search via Lévy flights, Nature & Biologically Inspired Computing, NaBIC 2009, World Congress on IEEE, 2009, pp.210-214.
[18] Karaboga, B. Basturk, A Powerful And Efficient Algorithm For Numerical Function

ACCEPTED MANUSCRIPT

Optimization: Artificial Bee Colony (ABC) Algorithm, J. Global Optim. **(**39)3 (2007) 459-471.
[19] W.T. PanA, new fruit fly optimization algorithm: taking the financial distress model as an example, Knowl. Based Syst. 26 (2012) 69-74.
[20] S. Kirkpatrick, C.D. Gelatt, M.P. Vecchi, Optimization by simulated annealing. Sci. 220 (4598) (1983) 671-680.
[21] S.I. Birbil; S. Fang, An electromagnetism-like mechanism for global optimization, J. Global Optim. 25(3) (2003) 263-282.
[22] R.A. Formato, central force optimization: a new metaheuristic with applications in applied electromagnetics, Prog. Electromagn. Res. 77 (2007) 425-491.
[23] E. Rashedi, H. Nezamabadi-Pour, S. Saryazdi, GSA: a gravitational search algorithm, Inf. sci. 179(13) (2009) 2232-2248.
[24] K.F. Pál, Hysteretic optimization for the Sherrington–Kirkpatrick spin glass. Phys. A: Mech. Its Appl. 367 (2006) 261-268.
[25] Z. Bayraktar, M. Komurcu, J.A. Bossard, D.H. Werner, The wind driven optimization technique and its application in electromagnetics. IEEE Trans. Antennas Propag. 61(5) (2013) 2745-2757.
[26] D.H. Wolpert, W.G. Macready, No free lunch theorems for optimization, IEEE trans. evol. comput. 1(1) (1997) 67-82.
[27] S. Zou, A. Parr, Estimation of Dispersion Parameters for Two-Dimensional Plumes. Ground Water 31(3) (1993) 389-392.
[28] P. Sidauruk, A.H.D. Cheng, D. Ouazar, Ground water contaminant source and transport parameter identification by correlation coefficient optimization, Ground Water, 36(2) (1998) 208-214.
[29] Z. Wang, P. Xie, C. Lai, X. Chen, X.Wu, Z. Zeng, J, Li. Spatiotemporal variability of reference evapotranspiration and contributing climatic factors in China during 1961–2013, J. Hydrol. 544 (2017) 97-108.
[30] X. Cao, G. Roy, W.J. Hurley, W.S. Andrews, Dispersion coefficients for Gaussian puff models, Boundary-Layer Meteorol. 139(3) (2011) 487-500.
[31] O.A. Cirpka, P.K. Kitanidis, Theoretical basis for the measurement of local transverse dispersion in isotropic porous media, Water Resour. Res. 37(2) (2001) 243-252.
[32] I.D. Benekos, O.A. Cirpka, P.K .Kitanidis, Experimental determination of transverse dispersivity in a helix and a cochlea, Water Resour. Res. 42(7). (2006) 1-10.
[33] X. Liu, A. Godbole, C. Lu, G. Michal, P. Venton, Optimization of dispersion parameters of Gaussian plume model for CO2 dispersion, Environ. Sci. Pollut. Res. 22(22) (2015) 18288-18299.
[34] S. Zou, A. Parr, Two-Dimensional Dispersivity Estimation Using Tracer Experiment Data. Ground Water, 32(3) (1994) 367-373.
[35] W. Yaoguo, L. Yunfeng, Complex Form Approximation for Determination of Hydrodynamic Parameters of Ground water Pollution, Shanghai Environ. Sci. 20(12) (2001) 586-588.
[36]J.J. Jiao, Data-Analyses Methods for Determining Two-Dimensional Dispersive Parameters, Ground Water 31(1) (1993) 57-62.
[37] J. Zhang, W. Wang, S. Han, Identifying aquifer parameters based on the decimal strings genetic algorithm, North West. Geol. 38(3) (2005) 100-104.
[38] M. Wang, G. Zhu, S. Jiang, Application of PSO in Inverse Calculation of Hydrogeological Parameters, Site Invest. Sci. Technol. 5(2007) 50-54.
[39] S.M. Jiang, G.R .Zhu, Z.B. Sun, X.J. Hu, Sequential uncertainty domain based on ant colony optimization for solving an inverse hydrogeologic problem, Hydrogeol. Eng. Geol. 34(3) (2007) 1-5.
[40] H. Goldstein, C.P. Poole, J.L. Safko, Classical Mechanics, Addison Wesley, Boston, 2001**.**
[41] J.P. Ryckaert, G. Ciccotti, H.J.C. Berendsen, Numerical integration of the cartesian equations of motion of a system with constraints: molecular dynamics of n-alkanes, J.Comput. Phys. 23(3) (1977) 327-341.
[42**]** R. Zheng, Z. Wu, Situ Measurement Method of Dispersion Coefficients for Groundwater, Environ. Sci. 9(2) **(**1988) 64-69.
[43] J.E. Nash, J.V. Sutcliffe, River flow forecasting through conceptual models, J. Hydrol. 10

ACCEPTED MANUSCRIPT

(1970) 282-290.

ACCEPTED MANUSCRIPT

ACCEPTED MANUSCRIPT

Liying Wang received the PhD. degree from Beijng Jiaotong University, China in 2014. Now she is an associate professor and works in Hebei University of Engineering. Her current research interests include intelligent computing, control systems engineering and water dynamics.

ACCEPTED MANUSCRIPT

ACCEPTED MANUSCRIPT

Weiguo Zhao received the PhD. degree from School of Electrical Engineering, Hebei University of Technology in 2016. Currently he is an associate professor in Hebei University of Engineering, his research interests include intelligent computing, intelligent fault diagnosis and water dynamics.

ACCEPTED MANUSCRIPT

ACCEPTED MANUSCRIPT

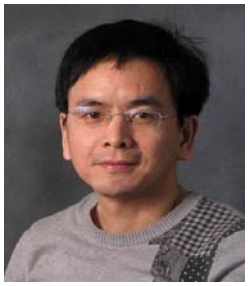

Zhenxing Zhang is a hydrologist with the Prairie Research Institute, University of Illinois at Urbana-Champaign, focusing on integrate water management, surface water supply, water availability, hydrologic modeling and stochastic hydrology. Dr. Zhang receives his Bachelors of Science in environment science from Wuhan University, Masters of Science in environment science from Peking University, and Masters of Science in applied statistics from University of Syracuse. He holds a Ph.D. degree in water resources engineering from the State University of New York College of Environmental Science and Forestry (SUNY ESF). He is a licensed Professional Engineer (P.E). He has published over 30 papers in top journals including Water Resources Research, Journal of Hydrology, Applied Energy, and Desalination.

ACCEPTED MANUSCRIPT

ACCEPTED MANUSCRIPT

•A novel optimization algorithm called Atom Search Optimization (ASO) is proposed.

The ASO is applied to dispersion coefficient estimation problem in groundwater.

•The results on dispersion coefficient estimation confirm the competitiveness of ASO.

ACCEPTED MANUSCRIPT